Effect of Lipase on Monoolein-Based Cubic Phase Dispersion (Cubosomes) and Vesicles

Johanna Borné, Tommy Nylander, and Ali Khan*

Physical Chemistry 1, Lund University Center for Chemistry and Chemical Engineering, Lund University, P.O. Box 124, SE-221 00 Lund, Sweden

Received: April 22, 2002; In Final Form: July 29, 2002

The effect of adding a *Thermomyces* (formerly *Humicola*) *lanuginosa* lipase (TLL) to a cubic dispersion of the binary monoolein (MO)−^2H_2O system and to vesicles formed by the ternary MO-sodium oleate (NaO)−^2H_2O system at high water content has been studied. The change in lipid aggregate structure during the lipolytic process was observed by light microscopy, cryo-TEM, and dynamic light scattering, and the lipid composition was determined with HPLC. The sequence of lipid aggregate structures observed upon lipase addition to the cubic dispersion is cubic dispersion → reversed cubic, hexagonal, and lamellar structures → large polygonal structures → dispersed oil droplets. The addition of lipase to MO/NaO aqueous-based vesicles did not change the morphology significantly. However, close to steady state, the vesicles changed from having smooth interfaces to irregular ones. When lipolysis reached steady state, the MO/(OA+NaO) ratio was similar in the two systems studied, although the morphology of the structures formed during lipolysis differed significantly. These differences are discussed in relation to the degree of dissociation of the fatty acid.

Introduction

It has been suggested that cubic liquid crystalline (lc) phases, especially the bicontinuous cubic lc structures, play a significant role in biological systems.[1−4] These structures appear during the lipolysis of triolein (TO) in vitro and in vivo, in addition to the initially occurring lamellar (L_α) lc phase.[5] Apart from micelles formed in the presence of bile salts, it has also been suggested that lc phases[6] and unilamellar vesicles[7] are important for the digestion and absorption of long-chain triacylglycerol in the gastrointestinal tract. Of particular interest are the monoacylglycerides and fatty acids/soaps which, together with bile salts, are essential for formation of such structures.[7] Unilamellar vesicles are thought to originate from L_α liquid crystals that form at the diacylglyceride/triacylglyceride emulsion interface during hydrolysis in the upper small intestine.[8] In a recent study of the ternary MO−sodium oleate (NaO)−^2H_2O system, different vesicle structures were found to be formed spontaneously at high water contents by diluting cubic and L_α phases.[9] In addition, vesicle formation has been reported in the OA−NaO−aqueous system, which was observed using various electron microscopy techniques.[10−12]

Dispersions of a cubic lipid−water phase were first discovered by Larsson et al.[1] In analogy with liposomes, these particles were termed cubosomes. The stability of cubosomes, formed in MO−H_2O-based systems, and the corresponding dispersed H_{II} phase (hexosomes) in the MO−TO−H_2O system was found to increase in the presence of an amphiphilic block copolymer (poloxamer).[13−15]

The effect of lipase action on MO−^2H_2O-based cubic lc phases in relation to lipid self-assembly has been reported previously.[16−20] In the present study, we focused on how *Thermomyces* (formely *Humicola*) *lanuginosa* lipase (TLL) affects the structures of dispersed cubic and lamellar phases in the water-rich corner of the MO−^2H_2O and MO−NaO−^2H_2O systems. The reason for choosing these two systems is 3-fold.

(I) Cubosomes and vesicles are formed from the corresponding lc phases. The dispersed structure of cubic phases (cubosomes) and L_α phases (vesicles) are two dominating types of structures formed when the corresponding lc phases are in an excess of water.

(II) The self-assembly structure in the MO/OA aqueous system is strongly dependent on pH. The two systems chosen represent different pH, slightly acid or neutral with pure MO and alkaline in the presence of NaO. The pH has previously been shown to strongly affect the phase behavior of aqueous MO−oleic acid systems.[21]

(III) Cubosomes and vesicles are formed during the lipolysis of acylglycerols in aqueous dispersions. Apart from micelles, these are most prominent structures formed during the lipolytic process.

The systems studied are rather polydisperse as are most biologically and technically relevant lipase substrates. This is particularly apparent in the vesicle sample, which was prepared by only mixing the components (without extrusion or sonication). In some applications, the homogenization of lipid dispersion is employed to reduce polydispersity; therefore, we also investigated the effect of extrusion of the vesicle sample. To cover the whole size range of dispersed aggregates, the structural characterization of solutions and dispersions in the present study was made from direct imaging by light microscopy as well as cryogenic transmission electron microscopy (cryo-TEM). Cryo-TEM allowed us to follow the lipolytic process as a function of time because the sample preparation method allowed us to instantaneously vitrify the specimens. Complimentary measurements of change in size of the dispersed aggregates (vesicles) because of lipase action were carried out with dynamic light scattering (DLS). High-performance liquid chromatography (HPLC) was used to determine the lipid composition of the different samples before and after lipase addition.

* To whom correspondence should be addressed. Fax: + 46 46 2224413. Phone: + 46 46 2223247. E-mail: ali.khan@fkem1.lu.se.

10.1021/jp021023y CCC: $22.00
Published on Web 09/12/2002

Materials and Methods

Materials. Monoolein (MO) Rylo Mg 90-glycerol monooleate (TS-ED 173; Journal no. 1876−88) was kindly provided by Danisco Ingredients (Braband, Denmark). The monoolein samples consisted of 95.7 wt % monoglycerides, 3.8 wt % diglycerides, 0.4 wt % free fatty acids, and 0.1 wt % free glycerol. The fatty acid composition was 90.0 wt % oleic acid, 5.0 wt % linoleic acid, 2.7 wt % stearic acid, 1.0 wt % palmitic acid, 0.3 wt % linolenic acid, and 1.0 wt % other fatty acids. Sodium oleate (purity >99%) was obtained from Nu-Chek-Prep, Inc., USA. The deuterated water (>99.8%) was obtained from Dr. Glaser AG (Basel, Switzerland). All of these chemicals were used as received. *Thermomyces* (formely *Humicola*) *lanuginosa* lipase (TLL) was obtained from Novozymes A/S, Denmark, and has a molecular weight of 32 000 g/mol. The lipase stock solution (1 mg/mL) was dialyzed against a 0.1 M sodium phosphate buffer, pH 8, for 36 h.

Sample Preparation. Binary MO−^2H_2O (2 wt % MO− 98 wt % ^2H_2O) and ternary MO−NaO−^2H_2O (1 wt % MO, 1 wt % NaO, and 98 wt % ^2H_2O) samples were prepared by weighing appropriate amounts of MO, NaO, and deuterated water in sample tubes ($\phi = 1.5$ cm). The sample size was about 4000 mg. They were then gently mixed in a rocking shaker at 25 °C for one week to ensure equilibration of the samples. The macroscopic appearance of the samples remained more or less unchanged when left for longer equilibration times.

The binary MO−^2H_2O sample appeared as a white dispersion coexisting with an isotropic gellike particle. The isotropic particle was removed prior to lipase addition to the white dispersion.

The ternary MO−NaO−^2H_2O sample separated into a denser top phase and a bluish bottom phase. Before carefully removing the top phase with a syringe, the sample was centrifuged at 2900 × g at 25 °C for 1 h. The bottom phase was sampled after removing the top phase. Lipase was added to both the top phase and the bottom phase.

In addition, three extruded ternary samples were prepared by passing an equilibrated sample repeatedly through two 13 mm polycarbonate filters with a nominal pore diameter of 100 nm (25 times) by means of a microsyringe. Two samples, one with and one without lipase, were, agitated on a rocking shaker for 12 h, whereas the remaining third sample was not agitated. The two samples without lipase were investigated in order to reveal the effect of agitation. Within 1−2 days after preparation, no visible phase separation was observed in the extruded reference samples.

The lipolytic process was initiated by adding 10 μL lipase solution (1 mg/ml) to 590 μL dispersions/solutions giving a final lipase concentration of 521 nM. The samples were thoroughly mixed in a rocking shaker at 25 °C and examined at different times after lipase addition.

Optical Polarizing Microscopy. An Axioplan Universal polarizing light microscope from Carl Zeiss, equipped with a differential interference contrast (DIC) unit, was used to identify anisotropic liquid crystalline phases based on the observed textures.[22−24] The technique is effective in the visualization of large vesicular structures. The disadvantage of the use of visible light is that it places a limit on the resolution. However, the use of DIC lenses enhances the contrast between the object and the background and allowed a resolution down to 0.5 μm. Samples for light microscopy were prepared by gently pressing a droplet between a slide and a cover slip. Photographic images of the textures were recorded with an Olympus (MC 100) camera.

Cryo Transmission Electron Microscopy (cryo-TEM). The cryo-TEM method[25,26] was used for direct imaging of samples in the dilute corner of the phase diagram. Vitrified samples were prepared and imaged according to a procedure described previously.[9] A Philips CM 120 BioTwin microscope specially designed for handling cryo-samples was used to image the samples.

Small-Angle X-ray Diffraction (SAXD). SAXD was performed on a modified version of the NanoStar small-angle X-ray equipment (Anton Paar, Graz, Austria) at the University of Aarhus, Denmark. The instrument was equipped with a powerful rotating anode X-ray source (Cu Kα, 0.3 × 0.3 mm^2 source point, 6 kW power) and a pinhole camera with two Göbel mirrors for monochromatizing and focusing the beam. The data were collected by a two-dimensional position-sensitive gas detector (HiSTAR).

Light Scattering. Dynamic light scattering (DLS) measurements were performed at room temperature (23 °C ± 0.02 °C). Approximately 1 mL of the solution was filtered through a membrane (Minisart, Sartorius 0.45 μm) to remove dust particles before it was transferred to the scattering cell. Measurements were made with an ALV goninometer instrument (ALV/DLS/SLS-5000F near-monomodal fiber compact goninometer system with an ALV 5000F fast correlator, ALV Laser Vertriebsgesellschaft, Langen, Germany), equipped with diode-pumped solid-state (DPSS) laser (model 532-400, Coherent Laser Group, Santa Clara, CA) operating at a wavelength of 532 nm. The DLS experiments were conducted at a scattering angle $\theta = 90°$. The measured DLS data were evaluated by the ALV-5000/E/win software to obtain the size distribution using an inverse Laplace transformation of the normalized intensity correlation functions ($g^{(2)}(t)$). The apparent hydrodynamic radius was calculated from the Stokes−Einstein equation assuming spherical geometry.

High-Performance Liquid Chromatography (HPLC). The HPLC system consisted of Gilson 305 and 306 pumps, a Gilson 805S manometric module, and a Gilson 811C dynamic mixer. A Sedex 45 evaporative light scattering detector (ELSD), operating at 40 °C and 2.5 bar, was used as detector. The gain was set at 8. The integrator was a Shimadzu C−R6A Chromatopac Reporting integrator. The column used was a HiChrom ACE−5 C18, 250 × 3.2 mm maintained at room temperature. The flow rate was 0.8 mL/min. Solvent mixture A consisted of water−MeCN−HAc (5:95:0.2 by vol.) and solvent mixture B consisted of EtOAc−HAc (100:0.2 by vol.). All samples were dissolved in solvent mixture A prior to analysis, diluting the samples by a factor of 20. A binary gradient was run according to the following scheme: time 0 min (t_0) − 0% B, t_2 − 0% B, t_{14} − 85% B, t_{15} − 85% B, t_{19} − 0% B, t_{30} − 0% B. The samples were injected using a Gilson 234 autosampler equipped with a 20 μL loop. Standard curves of high-purity MO, OA, and DO were obtained by injecting serially diluted standards (about 8−500 ng/μL). These curves were used to calculate the concentrations of the compounds in the samples. The error in the determined concentrations was about 5%.

Results

Effect of Lipase on Cubic Liquid Crystalline Dispersion. *Morphology before Addition of Lipase.* Cryo-TEM images of the binary MO−^2H_2O sample before lipase addition are shown in Figure 1 parts a and b. The dispersed cubic phase in the two-phase region is apparent as nonspherical particles connected by lamellar tubules. The size of the particles varied, as can be seen when comparing Figure 1 parts a and b, but inverse Fourier

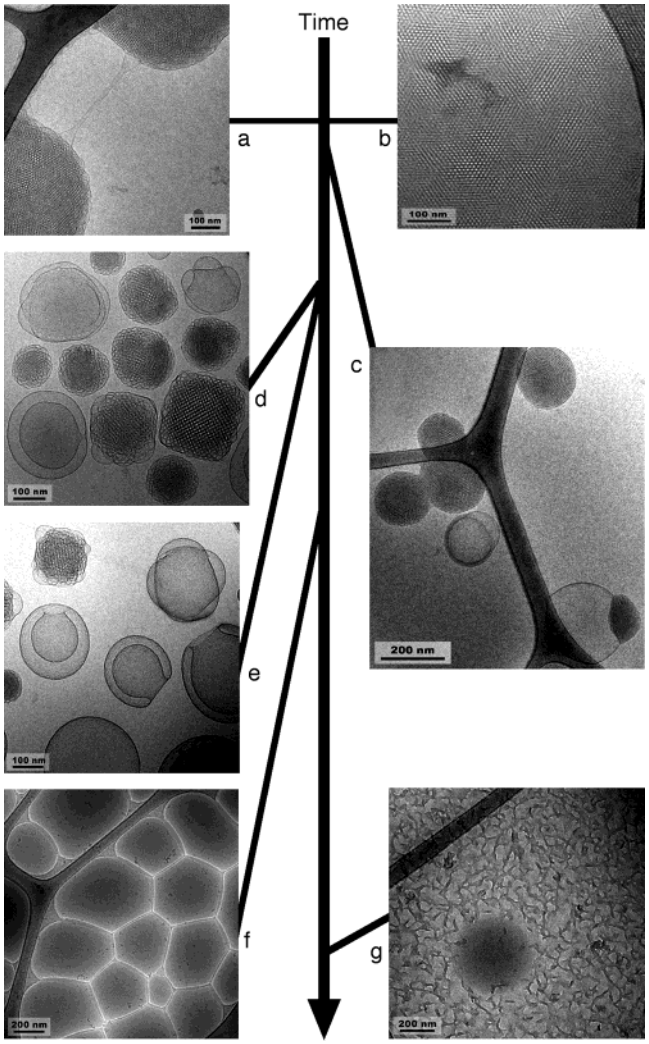

Figure 1. Cryo-TEM images of the MO−aqueous cubosome system before (a) and after (b−f) lipase addition. (a and b) Particles with an inner cubic structure connected to lamellar tubulues. (c) During the first 10 minutes, different reversed structures were seen in coexistence with different types of lamellar structures. for details see text. (d and e) After 1 h, cubosomes coexisted with spherical aggregates, with a seemingly less ordered inner structure, as well as different types of defect vesicle structures. For details, see the text. (f) After 2 h, large polygonal structures were observed. (g) After 8 h, as well as after 1 week, oil droplets were observed in a woven structure.

transformation of all of the images showed diffraction patterns of the same cubic structure (see discussion). The pH of the dispersion was determined to be 6.4, and the MO concentration was 10 mg/mL ($\sim$ 28 mM) obtained by HPLC. The molecular solubility of pure MO in water was found to be 10^{-7} M or 3.5×10^{-5} mg/mL. [27]

Time Dependent Changes in Morphology Due to Lipase Action. Lipase was added to the cubic dispersion, and cryo-TEM micrographs were recorded as a function of time to monitor the changes in the lipid aggregate structures induced by lipase action. A large number of grids were examined, and the reaction is illustrated by a sequence of representative micrographs in Figure 1. It should be noted that the observed effect of lipase action on different samples with similar compositions is highly reproducible.

Figure 1c demonstrates that the addition of lipase to the cubic lc dispersion brings about a dramatic change in microstructure during the first 10 min, which can be related to a decrease in the fraction of MO. The large particles with an inner cubic structure are fragmented and transformed into more or less spherical aggregates, most of them with a diameter of about 200 nm. The micrographs recorded show several coexisting microstructures. These are aggregates with both an inner cubic and hexagonal structure, different types of vesicles, and vesicles in close contact with parts of the original cubic structure.

After 1 h, we observed square-shaped particles (Figure 1 parts d and e) with an inner cubic structure (see discussion), also known as cubosomes.[1,13−15] The cubosomes coexist with spherical particles, with a seemingly less ordered inner structure. An inverse Fourier transformation of these dense inner structures did not yield any well-defined diffraction pattern. One reason for this may be that the spherical aggregates are composed of domains with different structures. Cubosomes and hexosomes often coexist with vesicles,[14,15] which is also evident in Figure 1 parts d and e. They also seem to be covered with a monolayer and/or bilayer of lipid, so as to keep them dispersed in aqueous solution. Not all of the vesicles are spherical, but some appear to be deflated, whereas others have interlamellar attachments. It is also notable that the size of all observed aggregates varies within the range 100−300 nm and that no vesicles with more than two bilayers were observed.

After 2 h, we observed large polygonal type structures (Figure 1f). Tightly packed vesicles are expected to give this kind of microstructure. Similar structures have also been observed for foams.

After 6 h, we observed spherical dark particles, with diameters in the range 75−250 nm, immersed in a woven structure (Figure 1g). The particles, which were found to be sensitive to radiation, are thought to be composed of OA and the woven structure might be the remains of the collapsed polygonal structure. The same morphology was observed after one week. However, the macroscopic appearance started to change slightly 8 h after lipase addition, and the sample seemed to be "creamier", indicating a coarser dispersion.

The results of the HPLC measurements, summarized in Table 1, show that the reaction was completed (reached steady state) within 5 h of lipase addition. Thus, it is clear that the changes in morphology observed with cryo-TEM reflect the changes in the sample composition. The final MO/(OA+NaO) molar ratio was 0.25, which means that 80% of the MO has been transformed into OA/NaO (Table 1). We noted that the HPLC analyses of the OA+NaO system were not reproducible because of the limited solubility of NaO in the solvent system used. Therefore, the analysis is based on the analysis of the MO concentration which was reproducible within $\pm$5%.

Effect of Lipase on the Vesicles. *Morphology before Addition of Lipase.* We reported previously that a sample with the composition 1 wt %MO, 1 wt %NaO, and 98 wt % ^2H_2O phase separated into a top and a bottom phase, where the volume of the top phase was less than 10% of the bottom phase. A high concentration of large polydisperse vesicles of different structures, e.g., spherical vesicles and tubular bilayer structures, were imaged in the top phase with light microscopy (Figure 2a). The size of the vesicles ranged from 1 to 50 μm. The cryo-TEM images showed disks as well as uni-, bi-, and multilamellar vesicles (10−800 nm) and tubular structures (Figure 2b). In the light microscope, the bluish bottom phase appeared to have a larger fraction of monodisperse, smaller vesicles than the top phase (Figure 2c). With cryo-TEM, we observed disks and a high concentration of small vesicles with diameters between 10 and 200 nm, but most frequently, diameters were between 10 and 70 nm (Figure 2d).

TABLE 1: Summary of the Result from the HPLC Analyses[a]

	before adding TLL	5 h after adding TLL			
sample	[MO]/mM	[MO]/mM	[OA+NaO]/mM	[MO/(OA + NaO)]	% MO hydrolyzed
cubic dispersion	28	5.6	22	0.25	80
top phase vesicle sample	73	32	41+92	0.24	56
bottom phase vesicle sample	29	11	18+37	0.20	64

[a] The OA+NaO concentration was calculated from the amount of hydrolyzed MO and added to the initial NaO+OA concentration. The initial MO/NaO+OA ratio in the ternary sample was assumed to be the same as the weighed proportions. This value was then used to calculate the OA+NaO concentration from the determined MO concentration.

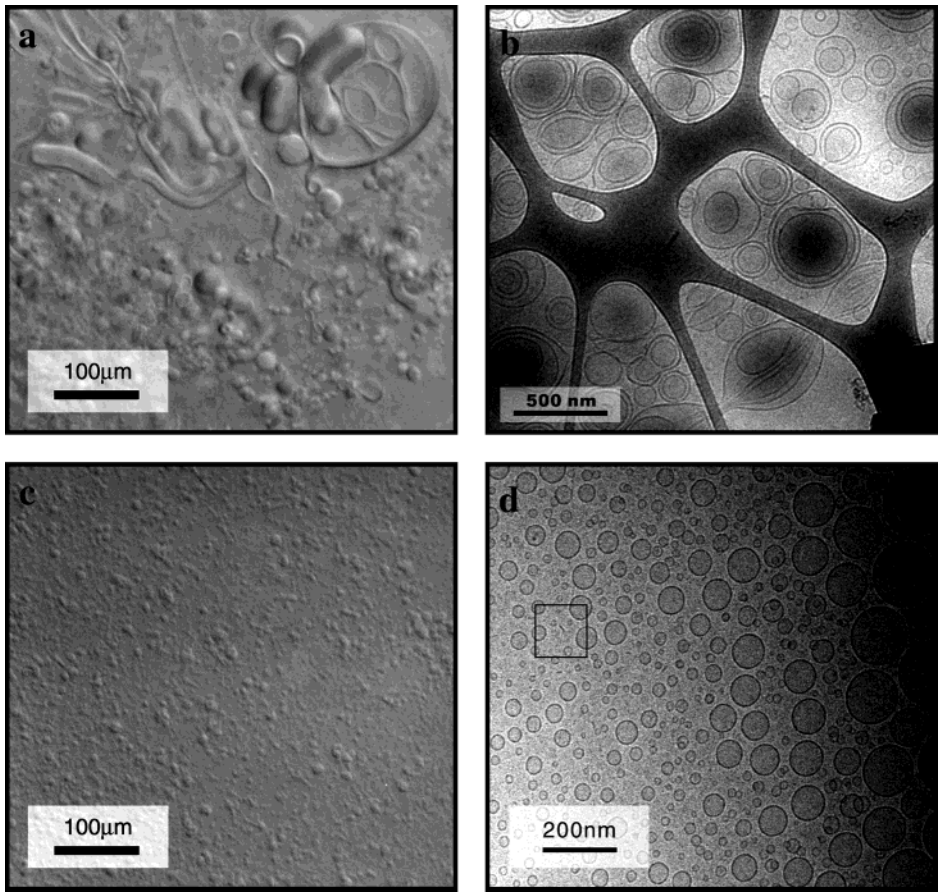

Figure 2. Light microscopy (a and c) and cryo-TEM images (b and d) of the MO/NaO aqueous vesicle system, where a and b show images of the top phase and c and d show the bottom phase.

The top phase, contains about 2.4 times more MO than the bottom phase (Table 1). It is notable that the initial pH in the ternary sample is 10.1 compared with 6.4 for the binary system. The extruded sample contains more monodisperse structures than the bottom phase, and no features could be observed with light microscopy. The majority of vesicles in the extruded sample had a size of less than 200 nm. Regarding the stability of the extruded vesicles, we found that they appeared unchanged within 24 h of preparation. However, after one week, this sample resembled that without extrusion; that is, it separated into a dense top phase and a bluish bottom phase.

Time-Dependent Changes in Morphology Due to Lipase Action. We added lipase to samples from the top and bottom phases as well as to the extruded sample. Apart from microscopic studies of the structural changes in all of the samples, DLS was also used to follow the changes in the extruded sample.

Macroscopic and Microscopic Appearance of the Top Phase. The micrographs in Figures 3 and 4 show the microscopic changes in the dense top phase after lipase addition. No notable change in the vesicle structure was observed with optical microscopy after 1 day. However, as the sample is highly concentrated and very polydisperse, changes in morphology may be difficult to observe. In fact, the cryo-TEM images in Figure 4 show nanoscopic changes in the vesicles in the top phase 3 h after lipase addition. These include the formation of the vesicle aggregates. At this high magnification, it was possible to view how the smooth bilayers of large vesicles transformed into more irregularly shaped vesicles with time. No further changes in the vesicles were observed with cryo-TEM after longer reaction times. The results of the HPLC measurements indicated changes in lipid composition within 5 h, after which the reaction reached steady state with the final lipid composition given in Table 1. The final MO/(OA+NaO) molar ratio decreased from 0.79, calculated from the given sample composition, to 0.24, which means that 56% of MO has been transformed into OA/NaO. It is also noteworthy that the pH in a mixture of top and bottom phase changed significantly from 10.1 to 9.5 within 2 h, and after 12 h, a value of 8.9 was measured.

Contrary to the results from the cryo-TEM and HPLC analysis, some changes were observed in the light microscope.

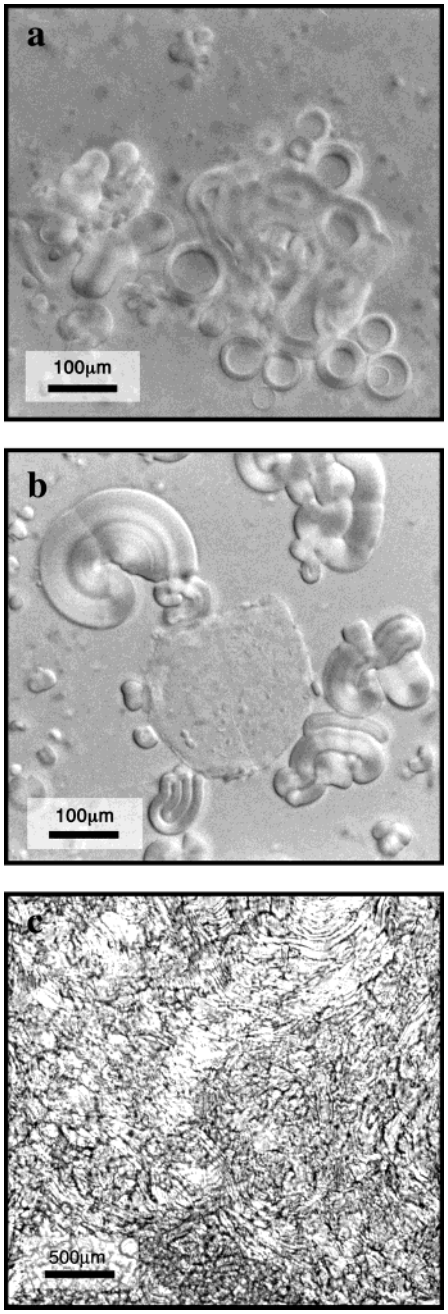

Figure 3. Light microscopy images showing the microscopic changes with time after lipase addition to the dense top phase of the sample shown in Figure 2a. (a) After 2 days, aggregation and formation of larger vesicles occurred. (b) After 5 days, the aggregation was even more obvious. (c) After 1 week, densely packed vesicles appeared.

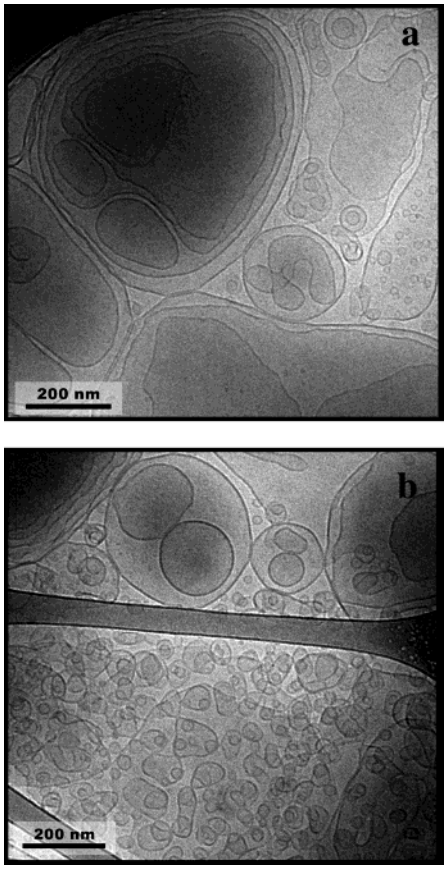

Figure 4. Cryo-TEM images, recorded 3 h after lipase addition to the dense top phase shown in Figure 2b. Large aggregated vesicles with an irregular interface can be seen.

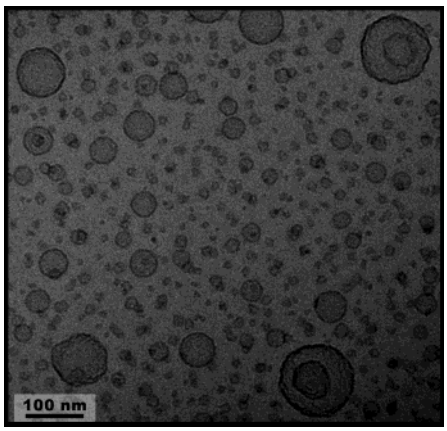

Figure 5. Cryo-TEM images recorded 12 h after lipase addition to bottom phase shown in Figure 2d show a few irregular vesicles with an inner structure in coexistence with spherical vesicles.

Some aggregation and the formation of larger vesicles occurred after 2 days (Figure 3a), and after 5 days, this aggregation was even more obvious (Figure 3b). After 1 week, the particles were so large that they could be observed by visual inspection. They appeared as densely packed vesicles in the microscope (Figure 3c). The top phase became more white/milky when the sample was left for even longer periods, although the white particles and the vesicles remained unchanged.

Macroscopic and Microscopic Appearance of the Bottom Phase. The transparent, bluish bottom phase became whitish in color when lipase was added. This indicates the formation of larger aggregates. However, no significant changes in size were observed with light microscopy or cryo-TEM, even after two weeks (Figure 2c). After 12 h, however, cryo-TEM images revealed that a few of the vesicles appeared irregular with an inner structure (Figure 5). These irregular vesicles remained unchanged over time. The results from the HPLC measurements indicated that the reaction reached steady state after 5 h. The final MO/(OA+NaO) molar ratio decreased from 0.79, as calculated from the given sample composition to 0.20, which means that 64% of the MO had been transformed into OA/NaO (Table 1). It is also notable that the pH decreased, as observed for the top phase.

Macroscopic and Microscopic Appearance of the Extruded Sample. Lipase was added to a 12-hour-old extruded sample (Figure 6). The cryo-TEM images recorded after a

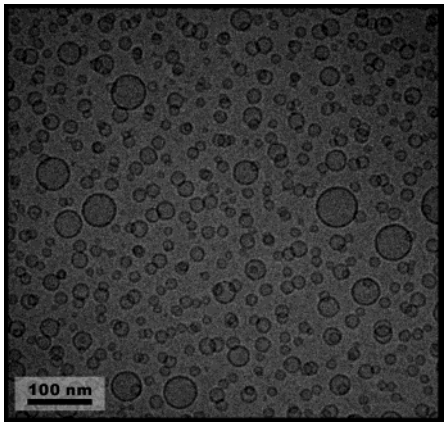

Figure 6. Cryo-TEM images of a vesicle sample with the composition 1 wt %MO, 1 wt %NaO, and 98 wt % ^2H_2O extruded through a filter with a nominal pore diameter of 100 nm.

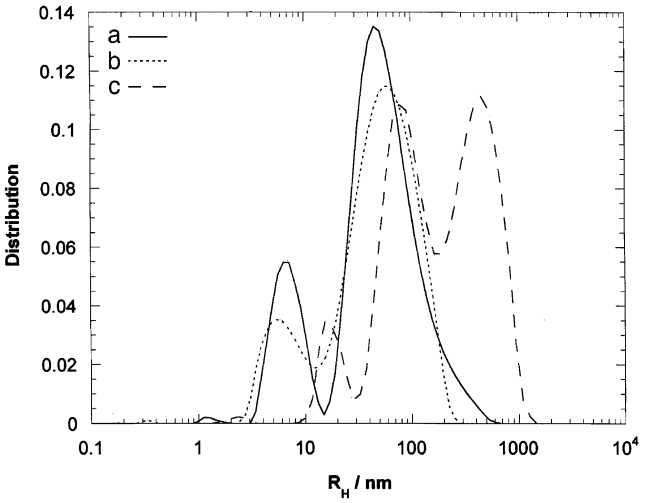

Figure 7. Dynamic light scattering spectra of extruded vesicle samples before and after lipase addition to the sample shown in Figure 6. (a) Nonagitated sample without lipase, (b) agitated sample without lipase, and (c) agitated sample with lipase.

further 12 h showed the same structures as those observed in the bottom phase after lipase addition (Figure 5).

Dynamic Light Scattering on the Extruded Sample. The size distribution of the extruded samples, calculated from DLS data, is shown in Figure 7. Three distinct peaks appeared for the nonagitated sample corresponding to average hydrodynamic radii of about 1−2, 6.5, and 43 nm. A similar size distribution was observed for a sample that had been subjected to agitation in a rocking shaker for 12 h, indicating that this type of agitation had a minor effect on the size distribution. After adding lipase, the size distribution changed significantly, with one peak at 15 nm, other at 77 nm, and a third at 450 nm. The two latter peaks overlapped to some extent.

Discussion

Cubosomes and Liposomes Are Formed from the Corresponding lc Phases. The ternary MO−NaO−^2H_2O and MO−OA−^2H_2O phase diagrams, described in detail previously,[9,21] are shown in Figure 8. The cubic liquid crystalline phase is in equilibrium with an excess of water in the binary MO−^2H_2O system, as well as in the ternary MO−NaO−^2H_2O system at a low content of NaO (i.e., 20 wt % of the lipid is NaO, which corresponds to a MO/NaO molar ratio of ≈2.8). In the binary MO−^2H_2O system, using the same batch of MO, the cubic phase

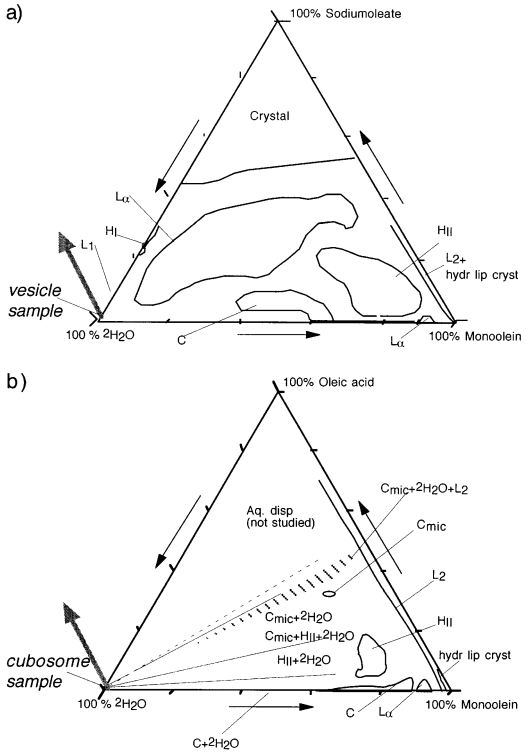

Figure 8. Ternary phase diagrams of (a) the MO−NaO−^2H_2O system and (b) the MO−OA−^2H_2O system at 25°. The phase notations are as follows: C, cubic phase; L_α, lamellar phase; L_2, reversed micellar solution phase; hydr. lip. cryst., hydrated lipid crystals; H_{II}, reversed hexagonal phase; H_I, normal hexagonal phase; C_{mic}, cubic micellar phase; aq. disp., aqueous dispersion. Composition is given in wt %.

was indexed to have the space group *Pn*3*m*, the diamond type of cubic phase (C_D),[1] with a lattice parameter (inner periodicity) of 91.5 Å.[28] As the cubosomes coexist with this C phase in the binary aqueous MO system, we assumed that they also had a C_D type of cubic structure. The diffraction pattern displays a cubic structure (Figure 9a), oriented along the (1,1,1) axis, with a lattice parameter of 118 Å if we assume that the cubic phase has a *Pn*3*m* space group. These findings were confirmed by high-resolution SAXD analyses of the cubosome sample, kindly provided by Prof. Jan Skov Pedersen (University of Aarhus, Denmark). This analysis gave a lattice parameter of about 126 ± 7 Å for the space group *Pn*3*m*, although the diffractogram obtained was quite weak for this highly diluted sample. Our values indicated a more swollen cubic phase compared with the findings of Gustafsson et al., who reported values of about 98 Å for a C_D cubic phase of MO in 80% water.[15]

As the ratio of MO to NaO decreased, the cubic phase was replaced with a large concentration range of L_α phase in equilibrium with water (Figure 8). Consequently, vesicles of different sizes and shapes in equilibrium with sheets of lamellar structure were formed spontaneously at high water content.[9] The vesicular structures dominate with excess water over a large range of MO/NaO ratio. However, micelles appear when 95 wt % of the lipid is NaO, corresponding to a MO/NaO molar ratio of ≈0.04. The initial concentration in our ternary sample corresponded to a MO/NaO molar ratio of 0.79. Therefore, vesicles dominated in our ternary sample, in both the top and bottom phase. This is apparent from the cryo-TEM and light microscopy images shown in Figure 4.

The Self-Assembly Structure in the MO/OA Aqueous System Is Strongly Dependent on pH. The intrinsic dissociation constant, pK_H, of soluble carboxylic acids is about 4.8, and

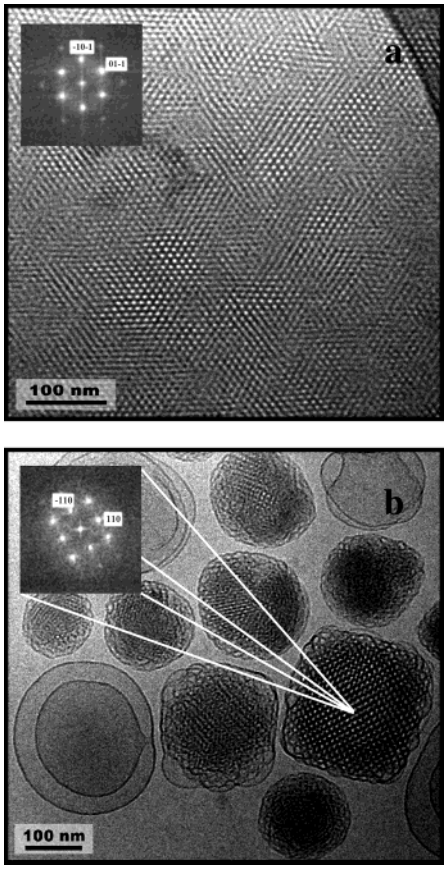

Figure 9. (a) Diffraction pattern displaying a cubic structure (Figure 1a), oriented along the (111) axis with a lattice parameter of 118 Å if the cubic structure is assumed to belong to the space group *Pn*3*m*. (b) Diffraction pattern that shows a cubic structure (Figure 1 parts d and e) oriented along the (001) axis with a lattice parameter of ∼145 Å, if we assume that the cubic phase belongs to the space groups *Pn*3*m* or *Im*3*m*.

a similar value, ≈5.0, has been estimated for isolated fatty acids in aqueous solution.[29] However, the apparent dissociation constant, pK_{aH}, may be quite different if the acid is incorporated into a lipid bilayer. Ptka et al.[29] reported pK_{aH}values of 7.2−7.4 for myristic and stearic acid incorporated into egg yolk phosphatidylcholine vesicles at a lipid concentration of 3.3 mol %, dispersed in 0.1 M phosphate buffer. The apparent dissociation constant, pK_{aH}, of the fatty acid in a self-assembly structure depends on electrostatic effects (ΔpK_{el}), i.e., the charge density at the interface and the ionic strength, and local effects (ΔpK_p), which include effects associated with the dielectric discontinuity created by the interface.[30,31] It is not easy to estimate the local effects as discussed by Cevc et al.,[30] and this is beyond the scope of the present study. The pK_{aH} can be expressed as:

$$pK_{aH} = pK_H + \Delta pK_{el} + \Delta pK_p$$

In the present study, the lipids were dispersed in pure water, and the ionic strength is thus low, and consequently, ΔpK_{el} is expected to be large. This means that the pK_{aH} values for our systems are likely to be significantly higher than the pK_{aH} values of 7.2−7.4 mentioned above. Unfortunately, to our knowledge, no data are available on pK_{aH} in the MO/NaO aqueous system. According to the data published by Cistola et al.[32] on the titration of potassium oleate, the titration curve of the oleate (OA^-) is quite complex. Three plateaus, where the pH is invariant with the amount of acid added, were observed at pH 9.0, 7.5, and 7.0. On the basis of these findings, we can say that a pK_{aH} of 9.0 represents the highest possible value of pK_{aH} for our system. We can then calculate the degree of ionization, *x*, under these conditions from

$$\log \frac{x}{1-x} = \mathrm{pH} - pK_{aH}$$

In the MO/NaO aqueous system, we observed a pH of 10.1 before lipase addition. For pK_{aH} = 9.0, this will give $x = 0.9$. After lipase addition, the pH decreased, to 8.9, giving $x = 0.4$ provided that the pK_{aH} remains at 9.0. These estimated values should only be taken as the lower limits for the degree of ionization. However, the fact that the pH decreases as fatty acids are formed, because of lipase action, shows that the fatty acids are at least partly dissociated. The pH of the MO−aqueous cubosome system increases only slightly, from pH 6.4 before lipase addition to 6.6 after the lipolytic reaction had reached steady state. This indicates a very low degree of dissociation of the fatty acids formed, which is consistent with a high pK_{aH}, =7.5, in the system studied. We also noted that the MO/(OA+OA^-) fraction is almost the same for the two systems after the lipolytic reaction reached steady state.

Self-assembly structures formed in the aqueous dispersion of fatty acids at different pH provide the reference point for understanding the formation of the structures observed in the MO/NaO aqueous system. Cistola et al.[32] were able to relate the different regions of the titration curve of potassium oleate, discussed above, to the formation of different self-assembly structures, as observed by SAXD, ^{13}C NMR, and polarizing light microscopy. Above pH 9, the fatty acid is completely dissociated and exists as a micellar solution. Mixtures of nondissociated acid and the corresponding soap form lamellar structures between pH 9 and 7. In the acid pH range (pH < 7), the acid is not dissociated, and the dominating structure is an aqueous dispersion of oil droplets. In later study on a similar system, Edwards et al. used cryo-TEM to examine how the aggregate structure in dilute solutions of oleic acid changed with the degree of dissociation of the fatty acid.[12] At pH 10.7, their cryo-TEM micrographs showed spherical or cylindrical micelles, depending on the concentration, whereas unilamellar vesicles existed at pH 9. Large clusters of aggregated vesicles coexisted with dispersed nonlamellar structure at pH between 8 and 7, indicating a reversed hexagonal structure. Nonlamellar liquid-crystalline structures and finally oil droplets were formed with decreasing pH and ionization.

These dramatic changes in the self-assembly structure due to changes in the degree of dissociation of the fatty acid are also apparent in the phase behavior of the MO−NaO−^2H_2O and MO−OA−^2H_2O ternary systems (Figure 8). The phase behavior of the ternary MO−NaO−^2H_2O system shows similar types of morphologies as observed for the aqueous dispersions of OA at pH = 7.5, whereas the ternary system containing the undissociated acid corresponds to the aqueous dispersions of OA at pH < 7.5. Here, we should take into account the fact that MO promotes structures with reversed curvatures toward the aqueous region (e.g., reversed bicontinuous cubic phase), whereas the dissociated OA promotes structures with normal curvature toward the aqueous region (e.g., micelles).[32] Mixtures of MO and NaO should give structures between those with reversed and normal curvature if the NaO is fully dissociated and the type of structure depends on the MO/NaO ratio.[9,21] Indeed, we observed that lamellar structures dominated when less than 95 wt % of the lipid was NaO, corresponding to a MO/NaO molar ratio of ∼0.04, whereas micelles appear at lower MO/NaO molar ratio. The dispersion of MO/NaO (molar ratio

~0.86) in aqueous solution before lipase addition had a pH of about 10, and as discussed above, OA is likely to be dissociated. Vesicles are therefore observed as the dominating structure.

Cubosomes and Vesicles Are Formed during Lipolysis of Acylglycerols in Aqueous Dispersions. *Effect of Lipase on Cubic Liquid Crystalline Dispersion.* During the initial stages of lipolysis, the cubic liquid crystalline dispersion is transformed into square-shaped aggregates with an inner cubic structure (Figure 1 parts d and e). These particles are similiar to the cubosomes reported by Larsson and co-workers.[1,13−15] In their studies, amphiphiles stabilized the cubosomes. It is possible that the OA/NaO formed during lipolysis might act as a stabilizer. In the ternary MO−OA−^2H_2O system, the gyroid (C_G) type of cubic phase exists in an excess of water at a MO/OA molar ratio below ~100. At this composition, which gives maximum swelling of the C_G phase (space group *Ia*3*d*), the lattice parameter is about 141 Å. The diffraction pattern, obtained by inverse Fourier transformation of the corresponding cryo-TEM image, indicates a cubic structure oriented along the (001) axis (Figure 9b). The lattice parameter would be 145 Å, if we assume that the cubic phase belongs to the space group *Pn*3*m* or *Im*3*m*. The space group *Im*3*m* corresponds to a primitive (C_P) type of cubic phase,[1] which has been observed at high water content in MO−aqueous systems with a third component such as DSPG (distearoylphosphatidylglycerol).[33,34] If we instead assumed the *Ia*3*d* space group (C_D phase), the lattice parameter would be 280 Å. Unfortunately, it was not possible to run high-resolution SAXD on this sample, and we could therefore not unequivocally determine the type of cubic structure.

The formation of hexosomes, where the lipid-aqueous interface has a more reversed curvature than in the cubic phase,[1] was observed after lipase addition. This is not surprising as the H_{II} phase is the dominating structure in the ternary MO/OA aqueous system. In addition to cubosomes and hexosomes, spherical particles, with a seemingly less ordered inner structure appeared. These spherical particles may be a dispersed sponge (L_3) phase, which is a disordered cubic phase. Dispersed L_3 phases have previously been observed in the MO−cetyltrimethylammonium bromide (CTAB)[35] and the MO−sodium cholate aqueous systems.[36]

As the lipolytic process proceeds, defect vesicles such as vesicles with interlamellar attachments (ILAs) and deflated vesicles were observed. Similar types of structures have been observed in the MO−CTAB[37] and in the MO−sodium cholate aqueous systems.[36] Interestingly, these types of defect vesicles were found to be the intermediate structures between the reversed structures, e.g., cubsomes, and vesicles in the ternary MO−NaO−^2H_2O system.[9] However, no intact vesicles were observed during lipolysis. As the lipolytic process approaches steady state, the structure collapses into oil droplets. Such droplets have been observed for pure OA in aqueous dispersions at pH < 7[12,32] as well as in the ternary MO/OA aqueous system at MO/OA molar ratios above about 0.9.[21] The observed structures indicate that the fatty acid formed during the lipolytic process on the dispersed cubic phase is not fully dissociated as discussed in the previous section. We also noted that when the lipase acts on a MO-aqueous based cubic phase at low water content (about 40 wt %), the reaction sequence in terms of phase transitions follows the order bicontinuous cubic → reverse hexagonal → micellar cubic → micellar phase.[19,20] This is in accordance with the MO/OA aqueous ternary system.[21]

Finally, we noted that the phase polymorphism observed during the lipolysis suggests an uneven distribution of the components.

Effect of Lipase on the Vesicles. The morphology of the ternary MO/NaO aqueous sample did not change very much during the lipolytic process; that is, vesicles were the dominating structure until the process reached steady state. This is, as discussed in detail above, expected from the phase behavior of the ternary MO/NaO aqueous system, bearing in mind that the pH of the dispersion varies between 9 and 10 during the lipolysis process.

The change from a smooth bilayer interface to irregular ones and the variety in lamellar structures observed in the top phase (Figure 4) are probably due to an increase in NaO:MO ratio. This promotes the formation of structures with a different curvature, e.g., the H_I phase. The irregular vesicles might also be due to lateral phase separation, e.g., the formation of domains enriched in OA/NaO, in the lipid bilayer as a consequence of the decrease in MO/(OA+OA^-) ratio. Such domains will invoke a locally different curvature and hence an irregular shape of the bilayer. It is noteworthy that a lamellar phase is known to form in the pure oleic acid system at a stoichiometry that ranges from approximately 1:1 to 1:3 between the associated and dissociated acid.[32]

The cryo-TEM images of the vesicles during lipolysis indicate that fusion occurs between the vesicles (Figure 4). This is visible as associated vesicles with a shared bilayer. Fusion can be regarded as intermediate between vesicles and reversed structures, e.g., inverted cubic and H_{II} phases (cf. refs 3, 38, and 39). The bottom phase of the vesicle sample during lipolysis is quite similar to the top phase in terms of morphology, although we did not observe any associated vesicles. This might be due to a 2.5 times lower lipid concentration in the former sample. In the bottom phase, we also observed some aggregates with a seemingly unordered inner structure. Such types of aggregates were also observed during the lipolysis of the dispersed cubic phase and might be a dispersed L_3 phase. Lipolysis of the extruded samples seems to give the same structural change as the ones observed for the bottom phase. This indicates that extrusion did not change the morphology, although a narrower size distribution was obtained. It was therefore meaningful to investigate this sample with DLS. The DLS data indicated an increase in the aggregate size during lipolysis. The observed changes are, however, difficult to quantify as the sample was rather polydisperse and DLS generally overestimates the contribution from larger aggregates relative to smaller ones.

Concluding Remarks

We have studied the effect of lipase on a lamellar (vesicles) and reversed structure (dispersion of cubic phase). The MO/(OA+NaO) ratio at steady state is similar in these two systems, although the morphology of the structures formed during lipolysis differs significantly. These differences can be related to the degree of dissociation of the fatty acid, which has a profound effect on the structures formed during the lipolytic process. It is important to stress that the action of the lipase only decreases the time taken to reach equilibrium and does not affect the equilibrium composition as such. Thus, the changes in structure and composition of the lipid dispersions reported in this work would have occurred without the lipase if given enough time. Such time-dependent changes in composition and structure have indeed been observed previously in MO-based aqueous systems.[21,40,41]

Acknowledgment. We are grateful to Alan Svendsen and Shamkant Patkar, Novozymes A/S, Denmark for the lipase sample and stimulating discussions, as well as Torsten Gun-

narson, Camurus AB, for his generous help with the HPLC analysis and Viveka Alfredsson for her valuable help and discussions concerning the indexing of the liquid crystalline structures imaged with cryo-TEM. Financial support was obtained from the EU Biotech Shared Cost Project, Contract No. BIO4-97-2365.

References and Notes

(1) Larsson, K. *J. Phys. Chem.* **1989**, *93*, 7304.
(2) Lindblom, G.; Rilfors, L. *Biochim. Biophys. Acta* **1989**, *988*, 221.
(3) Hyde, S.; Andersson, S.; Larsson, K.; Blum, Z.; Landh, T.; Lidin, S.; Ninham, B. W. *The language of shape. The role of curvature in Condensed matter: Physics, chemistry and biology*; Elsevier: Amsterdam, 1997.
(4) Luzzati, V. *Curr. Opin. Struct. Biol.* **1997**, *7*, 661.
(5) Patton, J. S.; Carey, M. C. *Science* **1979**, *204*, 145.
(6) Lindström, M.; Ljusberg-Wahren, H.; Larsson, K.; Borgström, B. *Lipids* **1981**, *16*, 749.
(7) Staggers, J. E.; Hernell, O.; Stafford, R. J.; Carey, M. C. *Biochemistry* **1990**, *29*, 2028.
(8) Hernell, O.; Staggers, J. E.; Carey, M. C. *Biochemistry* **1990**, *29*, 2041.
(9) Borné, J.; Nylander, T.; Khan, A. *J. Colloid Interface Sci.* **2002**, submitted.
(10) Gebicki, J. M.; Hicks, M. *Nature* **1973**, *243*, 232.
(11) Hargreaves, W. R.; Deamer, D. W. *Biochemistry* **1978**, *17*, 3759.
(12) Edwards, K.; Silvander, M.; Karlsson, G. *Langmuir* **1995**, *11*, 2429.
(13) Landh, T. *J. Phys. Chem.* **1994**, *98*, 8453.
(14) Gustafsson, J.; Ljusberg-Wahren, H.; Almgren, M.; Larsson, K. *Langmuir* **1996**, *12*, 4611.
(15) Gustafsson, J.; Ljusberg-Wahren, H.; Almgren, M.; Larsson, K. *Langmuir* **1997**, *13*, 6964.
(16) Luzzati, V.; Gulik, A.; DeRosa, M.; Gambacorta, A. *Chem. Scr.* **1987**, *27B*, 211.
(17) Mariani, P.; Luzzati, V.; Delacroix, H. *J. Mol. Biol.* **1988**, *204*, 165.
(18) Wallin, R.; Arnebrant, T. *J. Colloid Interface Sci.* **1994**, *164*, 16.
(19) Caboi, F.; Borné, J.; Nylander, T.; Khan, A.; Svendsen, A.; Patkar, S. *Colloids Surf., B* **2002**, *26*, 159−171.
(20) Borné, J.; Nylander, T.; Khan, A. *Langmuir* **2002**, accepted.
(21) Borné, J.; Nylander, T.; Khan, A. *Langmuir* **2001**, *17*, 7742.
(22) Rosevear, F. B. *J. Am. Oil Chem. Soc.* **1954**, *31*, 628.
(23) Rosevear, F. B. *J. Soc. Cosmet. Chem.* **1968**, *19*, 581.
(24) Ekwall, P. *Adv. Liquid Crysr.* **1975**, *1*, 1.
(25) Vinson, P. K. "Cryo-TEM, carbon-coated holey film"; The 45th Annual Meeting of the Electron Microscopy Society of America, 1987, San Francisco.
(26) Bellare, J. R.; Davis, H. T.; Scriven, L. E.; Talmon, Y. J. *J. Electron Microsc. Technol.* **1988**, *10*, 87.
(27) Campos, J.; Eskilsson, K.; Nylander, T.; Svendsen, A. *Colloids Surf., B* **2002**, *26*, 172−182.
(28) Borné, J.; Nylander, T.; Khan, A. *Langmuir* **2000**, *16*, 10044.
(29) Ptka, M.; Egret-Charlier, M.; Sanson, A.; Boulossa, O. *Biochim. Biophys. Acta* **1980**, *600*, 387.
(30) Cevc, G.; Sedon, J. M.; Hartung, R.; Eggert, W. *Biochim. Biophys. Acta* **1988**, *940*, 219.
(31) Engblom, J.; Engström, S.; Jönsson, B. *J. Controlled Release* **1998**, *52*, 271.
(32) Cistola, D. P.; Hamilton, J. A.; Jackson, D.; Small, D. M. *Biochemistry* **1988**, *27*, 1881.
(33) Razumas, V.; Talaikyté, Z.; Barauskas, J.; Larsson, K.; Miezis, Y.; Nylander, T. *Chem. Phys. Lipids* **1996**, *84*, 123.
(34) Engblom, J.; Miezis, Y.; Nylander, T.; Razumas, V.; Larsson, K. *Prog. Colloid Polym. Sci.* **2000**, *116*, 9.
(35) Gustafsson, J. Aggregate strucuture and phase behaviour in lipid-surfactant−water mixtures. Ph.D. Thesis, Uppsala University, Uppsala, Sweden, 1997.
(36) Gustafsson, J.; Nylander, T.; Almgren, M.; Ljusberg-Wahren, H. *J. Colloid Interface Sci.* **1999**, *211*, 326.
(37) Gustafsson, J.; Orädd, G.; Nyden, M.; Hansson, P.; Almgren, M. *Langmuir* **1998**, *14*, 4987.
(38) Siegel, D. P.; Burns, J. L.; Chestnut, M. H.; Talmon, Y. *Biophys. J.* **1989**, *56*, 161.
(39) Siegel, D. P.; Green, W. J.; Talmon, Y. *Biophys. J* **1994**, *66*, 402.
(40) Caboi, F.; Amico, G. S.; Pitzalis, P.; Monduzzi, M.; Nylander, T.; Larsson, K. *Chem. Phys. Lipids* **2001**, *109*, 47.
(41) Murgia, S.; Caboi, F.; Monduzzi, M.; Ljusberg-Wahren, H.; Nylander, T. *Prog. Colloid Polym. Sci* **2002**, *120*, 41−46.